

Optical displacement sensor (ODS), a LISA's inertial reference sensor candidate

Meng P. Chiao*, Frank Dekens, Alex Abramovici
Jet Propulsion Laboratory

ABSTRACT

We propose here an optical displacement sensor (ODS) as a supplemental or backup sensor for the LISA inertial reference sensor concept. This simple ODS consists of a laser diode and a quad-cell photodiode (both commercially available). The inertial mass' reflective surface directs the laser beam onto the quad-cell photodiode. Changes in the inertial mass' position and orientation are then extracted from ratios of the differences and sums of the quad-cell photodiode outputs. A simpler proto-type using a 200 microns wide slit has demonstrated a resolution of 10 nm/ $\sqrt{\text{Hz}}$ at 1 mHz and 1 nm/ $\sqrt{\text{Hz}}$ above 5 mHz. The electronics noise was 1 nm/ $\sqrt{\text{Hz}}$ at and above 1 mHz with simple and off the shelf electronics components. Although this ODS' current performance does not meet the LISA's system requirement¹ of 1 nm/ at 1 mHz, we think that is achievable in the near future.

Keywords: Displacement sensor, low frequency measurements

1. INTRODUCTION

One of LISA's technical challenges is to achieve drag-free control such that the proof mass experiences minimal or no spurious disturbances other than gravitational waves and in particular not from its surrounding spacecraft. The present baseline technology utilizes capacitive sensors and actuators to maintain the gap (nominally 2 cm from each face) between the cubic proof mass and the spacecraft housing. Given the stringent performance requirement of LISA, the read-out resolution in the sensitive direction is specified at 1 nm/ $\sqrt{\text{Hz}}$ at 1 mHz and may be extended down to 0.1 mHz¹. The control strategy and identification of disturbance sources remain topics of diligent studies and discussions. One particular concern is the effective electrostatic coupling associated with the use of capacitive sensors. With that in mind, an optical displacement sensor becomes a logical supplement or alternative.

Optical displacement sensors come in different configurations for various applications. A quick survey in literature identifies the following usage: a) in atomic force microscope, an interferometer sensor with a nominal 2×10^{-14} m/ $\sqrt{\text{Hz}}$ sensitivity at and above 2 kHz² and 7×10^{-12} m/ $\sqrt{\text{Hz}}$ sensitivity from 10 to 200 Hz³; b) in biomedical applications, a so-called optical follower with 10^{-7} m resolution at and below 20 Hz⁴ and a fiber-optic micrometer with an estimated sensitivity of 10^{-8} m at and below 3 Hz for an operating range of 50-500 microns⁵; and c) in the Laser Interferometer Gravitational-Wave Observatory (LIGO), a simple detection system using a split photodiode with 10^{-11} m/ $\sqrt{\text{Hz}}$ resolution at and above 1 Hz⁶. There has not been any demonstration of an optical displacement sensor applicable for the LISA inertial reference sensor.

We propose a simple optical displacement sensor for low frequency applications (whose concept is similar to that in the LIGO setup) using available technology. Several prototype configurations have demonstrated 10 or 20 nm/ $\sqrt{\text{Hz}}$ sensitivity at 1 mHz in the laboratory. We will present here the basic concept, laboratory prototype setups and various experimental results.

2. CONCEPT

We extended the basic concept of linear optical displacement detection using a split photodiode as conceived by Mike Zucker⁷ to a two-dimensional sensor using a quad-cell photodiode. A generic configuration of this ODS comprises a light source, a slit (for linear motion) or an aperture (for motion in two dimensions), and an electro-optic quad-cell

* meng.p.chiao@jpl.nasa.gov; phone 1 818 354-7878; fax 1 818 393-6984; Jet Propulsion Laboratory, 4800 Oak Grove Drive, Pasadena, CA, USA 91109-8099

photodiode (Fig. 1). Each element of the quad-cell photodiode generates a current proportional to the light intensity on the element. As a fixed intensity pattern moves, the photocurrents increase or decrease accordingly. Through transimpedance amplifiers, these currents become measurable voltages. A normalized dimensionless variable ξ is defined as the ratio of the differential signals relative to the sum total for normalization of an overall intensity variation. For the lateral dimension,

$$\xi = \frac{(V_A + V_D) - (V_B + V_C)}{(V_A + V_D) + (V_B + V_C)}, \quad (1)$$

and for the vertical dimension,

$$\xi = \frac{(V_A + V_B) - (V_C + V_D)}{(V_A + V_B) + (V_C + V_D)}. \quad (2)$$

Since a quad-cell photodiode is equivalent to a superposition of two orthogonal split photodiodes, for the sake of simplicity, the remaining theoretical discussion will be treated for a split photodiode. This is the linear motion configuration in Figure 1. Elements A and D combine as one of the split photodiode element (V_1), and B and C as the other (V_2). Now

$$\xi = \frac{V_1 - V_2}{V_1 + V_2}, \quad (3)$$

and ranges between -1 and 1. A straightforward geometric consideration leads to an optimal slit width equal to one half of the split diode element width. Consequently, the overall operating range can be twice the slit width plus the split photodiode width.

A small position change (δx) in the illumination pattern on the split diodes leads to corresponding intensity change (δI) and thus a voltage signal change ($\delta V \propto \delta I$). Near the null or balanced position where $\xi = 0$, in terms of the illumination intensity,

$$I_1 = \frac{I}{2} + \delta I \text{ and } I_2 = \frac{I}{2} - \delta I \quad (4)$$

where I is the total intensity, and thus

$$\delta \xi = 2 \frac{\delta I}{I}. \quad (5)$$

Therefore, the displacement can be obtained by using

$$\delta x = \frac{dx}{d\xi} \delta \xi = \frac{dx}{d\xi} \frac{2\delta I}{I} = \frac{dx}{d\xi} \frac{2\delta V}{V}. \quad (6)$$

The calibration factor $dx/d\xi$ is empirically determined. There is no restriction on the intensity profile, but any non-uniformity would modify the linearity of the calibration factor. Furthermore, an intensity distribution change in time will contribute as a noise or error source.

For LISA's inertia sensor application, we visualize a configuration using the proof mass surfaces as reflectors and three sets of ODS in mutually orthogonal orientations (Fig. 2). This will resolve the measurement degeneracy between the linear translations (in the line of sight of ODS) and rotations and definitively determine the relative displacements between the proof mass and the spacecraft in six degrees of freedom. We also recommend using a collimated light source in the ODS to make it more adaptive since the gap between the proof mass and the spacecraft is still a design parameter. The angle between the light source and the quad-cell photodiode can also be adjusted to accommodate the range of operation and sensitivity level.

3. EXPERIMENTAL SETUP

A generic configuration was used as the blue print for the development and understanding of this low frequency ODS in the laboratory (Fig. 1). We started with a LED, a 200 microns wide slit and a silicon quad-cell photodiode whose element size was 0.5 mm by 0.5 mm. Various illumination sources such as laser diodes and Nd:YAG lasers, fiber coupled or not, collimated or not, were considered together with different quad-cell photodiode sizes and materials. The slit was also changed to an aperture to approximate the LISA configuration. The quad-cell photodiode was mounted on a linear translation stage (with a resolution of 0.01 mm) for calibration purpose.

In all cases, the photodiodes were operated under no reverse bias voltage to avoid the dark current noise since reduction of detector capacitance and thus speed was of no consequence. We were interested in signals at and below 1 Hz. The photocurrents were sent through transimpedance amplifiers whose feedback resistors were adjusted at different illumination intensity levels to maintain voltage outputs adequate for the analog to digital converters (ADC). Low pass filters with a 3 dB cut-off at 1 Hz (double check) were inserted at the inputs to the ADC to minimize signal aliasing. A current supply was built for LEDs and laser diodes using a low noise reference voltage chip to minimize optical intensity fluctuations in time. The entire ODS setup including the amplifiers and the current supply circuit were enclosed before the measurements to reduce thermal fluctuations and air turbulence while employing thermistors to monitor the thermal trend (Fig. 3).

Calibration measurements were taken for each ODS condition whose data were then analyzed to obtain the calibration factor. The ODS sensitivity measurements were conducted near the null position, and the electronics noise was measured in the same setup without any illumination. Digitized data were collected via a PC and were analyzed using Matlab to obtain the power spectral density (PSD).

4. RESULTS AND DISCUSSIONS

We tabulate in this section a representative subset of our experimental results at 1 mHz. For the purpose of conciseness, listed below are explanations for the notations used in this section.

Notation	Explanation
Si	Si quad-cell photodiode, active area = $0.5 \times 0.5 \text{ mm}^2$, responsivity = 0.4 A/W at 630 nm
InGaAs	InGaAs quad-cell photodiode, active area = $0.5 \times 0.5 \text{ mm}^2$, responsivity = 0.4 A/W at 1300 nm
Ge	Germanium quad-cell photodiode, active area = $0.25 \pi 2.5 \times 2.5 \text{ mm}^2$, responsivity = 0.6 A/W at 1300 nm
LED	LED at 635 nm from HP
YAG	Nd:YAG laser at 1319 nm from LightWave, fiber coupled, collimated
LD1	Laser diode at 635 (?) nm from Thorlabs, collimated
LD2	Laser diode at 1300 nm with its own power supply, fiber coupled, collimated
LD3	Laser diode at 1550 nm from JDS Uniphase, single mode, fiber coupled, collimated
LD4	Laser diode at 1300 nm from Newport, single mode, fiber coupled, collimated
Modulated	10 mA amplitude current modulation at 100 kHz

A sample calibration data plot shows the linearity of the calibration factor, which is indicative of the quality of the light source, within the operating range and in the vicinity of the null position (Fig. 4). A fiber coupled optical attenuator or neutral density filters were used to adjust the final optical power while operating the light sources in their stable conditions. In general, the setup was enclosed some time before the start of measurements to equilibrate. A

measurement usually last about 10,000 seconds. Some were 40,000 seconds, and the longest was 360,000 seconds. The sampling rate was 0.1953 seconds/point for the 16-bit ADC, and 1.286 or 2 seconds/point for the 24-bit. For analysis of the electronics noise, the averages of the detector signals from the ODS measurements were added to the corresponding electronics noise measurements and thereby to simulate perfectly constant sources and detectors with only amplifier noise. The ODS sensitivity and electronics noise values were then estimated (allowing variation within a factor of 2) from their PSD plots (Fig. 5).

4.1 Light source

Measurements were performed using a 200 microns wide slit, transimpedance feedback resistors of 10 M Ω , and a 16-bit ADC with variable dynamic range to investigate the influence from different light sources.

Light source	Detector	Calibration factor (nm/(V/V))	Electronics noise (nm/ $\sqrt{\text{Hz}}$)	ODS sensitivity (nm/ $\sqrt{\text{Hz}}$)
LED	Si	240000	50	80
LD1	Si	115000	2	100
YAG	InGaAs	70900	1	30
LD2	InGaAs	70900	1	1000
LD3	InGaAs	70900	1	20
LD3, modulated	InGaAs	70900	1	200
LD4	InGaAs	70900	1	200
LD4, modulated	InGaAs	70900	1	20

The LED and LD1 setups had rather large calibration factors because of their divergence. Also because of the ADC resolution limit then, the LED case had a large electronics noise. In contrast, other measurements had 1-2 nm/ $\sqrt{\text{Hz}}$ electronics noise by use of a delta-sigma amplifier between the transimpedance amplifiers and the ADC and a small dynamic range. YAG, LD3, and modulated LD4 gave comparable sensitivity about 20 nm/ $\sqrt{\text{Hz}}$ at 1 mHz. This result provides an option when implementing this ODS as the LISA inertia reference sensor; the sensor can either use a laser diode as a completely separate subsystem in LISA or share the YAG laser source on board.

4.2 Aperture size

Measurements were conducted using the modulated LD4 as the light source, a Ge detector, transimpedance feedback resistors of 10 M Ω , and a 24-bit (at ± 10 V full scale) ADC for a comparison between the linear and two-dimension configurations. No delta-sigma amplifier was used between the transimpedance amplifiers and the ADC.

Aperture diameter (mm)	Calibration factor (nm/(V/V))	Electronics noise (nm/ $\sqrt{\text{Hz}}$)	ODS sensitivity (nm/ $\sqrt{\text{Hz}}$)
0.2 mm wide slit	76200	1	10
1.9	738500	10	40
3.06	995700	15	30
Full beam size	2068000	30	70

^a If the detector was rotated by about 15 degrees, the sensitivity improved to be 20 nm/ $\sqrt{\text{Hz}}$. We think the rotation might have reduced some interference due to back reflection at the detector window.

During these measurements, the optical intensity was adjusted to maintain comparable total optical power on the detectors or voltage signal levels around 6 V, so the smaller beam size corresponded to higher intensity. The ODS sensitivity values degraded slightly with the increase of the aperture size. We attributed this to the possible pointing instability inherent in the laser diode since the LD4 beam did not have a uniform profile. A much smaller aperture compared to the actual beam size when centered would have a more uniform profile and is less sensitive to pointing instability. The electronics noise scaled with the calibration factors as the aperture change in the absence of light should have no influence on the electronics.

4.3 Transimpedance amplifier feedback resistor

Measurements were taken using the modulated LD4 as the light source, an aperture whose diameter was 3.06 mm, a Ge detector, and a 24-bit (at ± 10 V full scale) to investigate the noise contribution from feedback resistors in the transimpedance amplifiers. No delta-sigma amplifier was used between the transimpedance amplifiers and the ADC. The calibration factor was 997200 nm/(V/V).

Feedback resistor (k Ω)	Electronics noise (nm/ $\sqrt{\text{Hz}}$)	ODS sensitivity (nm/ $\sqrt{\text{Hz}}$)	Estimated optical power (μW)
10000	15	30	4.24
510	7	30	79.65
49.5	8	15	307.74

During these measurements, the optical intensity was again adjusted to maintain comparable voltage signal levels around 6 V, but only about 2.28 V at 49.5 k Ω limited by LD4's available power. A smaller resistor value corresponded to a higher intensity. The ODS sensitivity was best for the 49.5 k Ω case with an estimated intensity of 4.185 mW/cm². This implies a better ODS sensitivity with a higher optical intensity. The electronics noise increased by a factor of 2 when the feedback resistor value increased from 510 k Ω to 10 M Ω , but it remained about the same level below 510 k Ω .

4.4 Noise considerations

An electronics noise limit due to the 24-bit ADC alone was first established by grounding its inputs. For comparison purpose, it was determined to be 3 nm/ $\sqrt{\text{Hz}}$ at 1 mHz using the calibration factor of 997200 nm/(V/V) from the 3.06 mm aperture case, which was our most recent measurement setup.

Using transimpedance amplifier feedback resistors of 10 M Ω , a series of measurements were taken in the absence of light to compare the electronics noise from different detectors in the absence of illumination.

Detector type	Electronics noise (nm/ $\sqrt{\text{Hz}}$)
Si	5
InGaAs	6
Ge	15
Input open	4
Capacitors across input terminals	4

Si and InGaAs detectors, which had the same active areas, had comparable electronics noise levels close to that from null inputs (which set the electronics limit). Although Ge had an active area approximately 20 times as large, its electronics noise was merely 3 times bigger. On the other hand, this noise increase could also be related to the semiconductor material. If the feedback resistors were decreased to 510 k Ω , the electronics noise remained at 4 nm/ $\sqrt{\text{Hz}}$ for zero inputs, but improved to 4 nm/ $\sqrt{\text{Hz}}$ for the InGaAs and 7 nm/ $\sqrt{\text{Hz}}$ for the Ge. A four times longer measurement further improved the electronics noise to 4 nm/ $\sqrt{\text{Hz}}$ for the Ge. In the mean time, the ODS sensitivity remained at 30 nm/ $\sqrt{\text{Hz}}$. In an effort to understand the almost factor of 10 difference, a low noise reference voltage source through a series 510 k Ω resistor was implemented to simulate a constant photodiode signals into the transimpedance amplifiers, and that gave a noise level of 10 nm/ $\sqrt{\text{Hz}}$.

Continuing our attempt to identify the noise contributors, a series of measurements were performed using this reference voltage source (set around 6 V) at various locations and 510 k Ω transimpedance feedback resistors.

Locations	Electronics noise (nm/ $\sqrt{\text{Hz}}$)
Directly teed to four ADC inputs	3
Through a voltage divider and then teed to four ADC inputs	6
Through a series 510 k Ω resistor to one amplifier whose output was then teed to four ADC inputs	5
Through four series 510 k Ω resistors to four amplifiers whose outputs were sent to four ADC inputs	5

This reference voltage did not appear to contribute additional noise since the noise level when it was sent directly to the ADC inputs was the same as ground inputs. Although through a voltage divider the noise was twice as big, that could be explained by the halved voltage signals at the ADC inputs given the same amount of voltage fluctuations. However, when the reference voltage was used indirectly as inputs to the transimpedance amplifiers, there was a slight increase in the noise level. During these measurements, we also noticed noise level change due to electrical contacts between the amplifier IC chip and its socket in the circuit.

To separate the electrical noise sources from the optical, we replaced the modulated LD4 by a high power IR LED. If it was positioned such that its beam was much bigger than the Ge detector, a uniform intensity profile across the detector became possible. Keeping the 510 kW transimpedance feedback resistors and 997200 nm/(V/V) calibration factor, the noise level was about 20 nm/ $\sqrt{\text{Hz}}$. Since the measurements were conducted after the IR LED had been on for several days, it was expected to be quite stable in time and in its intensity profile. It becomes our next puzzle to answer whether this was due to detector noise only or actual motions.

5. CONCLUSION

We have demonstrated in the laboratory ODS prototypes with 10-30 nm/ $\sqrt{\text{Hz}}$ sensitivity and nominally 4 nm/ $\sqrt{\text{Hz}}$ electronics noise at 1 mHz (Fig. 5). The present technology on ADC sets the experimental performance limit at 3 ppm/ $\sqrt{\text{Hz}}$, which suggests that the 24-bit ADC is at best 20-bit. Although the transimpedance amplifier is not specified at 1 mHz, it has been chosen because of its excellent performance at 1 Hz. As experiments have shown, it does not seem to contribute much noise with near zero inputs. It appears to have higher noise with non-zero inputs. Unfortunately, the quad-cell photodiode collection we now possess does not allow a definitive assessment. It would be worthwhile to find either large active area InGaAs detectors or small area Ge detectors for a better comparison. Finally, we plan to set up simultaneous measurements with an interferometer device to validate the ODS sensitivity.

Although the current ODS performance does not meet the LISA's stringent specification of 1 nm/ $\sqrt{\text{Hz}}$ at 1 mHz, we think we can reach that level of sensitivity in the near future. As it is, this performance surpasses the minimal sensor read-out requirement of 280 nm/ $\sqrt{\text{Hz}}$ at 1 mHz and 0.1 mHz under the most optimistic estimates of total disturbances⁸ and proves itself a viable inertia reference sensor candidate.

ACKNOWLEDGEMENTS

This work was carried out at the Jet Propulsion Laboratory, California Institute of Technology, under the contract with the National Aeronautics and Space Administration. The authors are particularly grateful to Jacob Chapsky for many insightful discussions.

REFERENCES

1. Final Technical Report of the (Phase A) study of the Laser Interferometer Space Antenna (Dornier Satellitensystem GmbH-matra marconi space -Alenia Aerospazio), ESTEC Contract No. 13631/99/NL/MS, Report No. LI-RP-DS-009 (April 2000).
2. D. Rugar, H.J. Mamin, R. Erlandsson, J.E. Stern, and B.D. Terris, "Force microscope using a fiber-optic displacement sensor", *Rev. Sci. Instrum.*, **59** (11), 2337-2340, November 1988.
3. M. Sasaki, H. Kazuhiro, S. Okuma, M. Hino, and Y. Bessho, "Improved differential heterodyne interferometer for atomic force microscopy", *Rev. Sci. Instrum.*, **65** (12), 3697-3701, December 1994.
4. S.W. Moore, "A fiber optic system for measuring dynamic mechanical properties of embryonic tissues", *IEEE Transactions on Biomedical Engineering*, **41** (1), 45-50, January 1994.
5. W.H. Ko, K.-M. Chang, G.-J. Hwang, "A fiber-optic reflective displacement micrometer", *Sensors and Actuators A* **49**, 51-55, 1995.
6. D.B. Newell, S.J. Richman, P.G. Nelson, R.T. Stebbins, P.L. Bender, J.E. Faller, and J. Mason, "An ultra-low-noise, low-frequency, six degrees of freedom active vibration isolator", *Rev. Sci. Instrum.*, **68** (8), 3211-3219, August 1997.

7. Mike Zucker, private communication.
8. B.L. Schumaker, "Overview of disturbance reduction requirements for LISA", private communication.

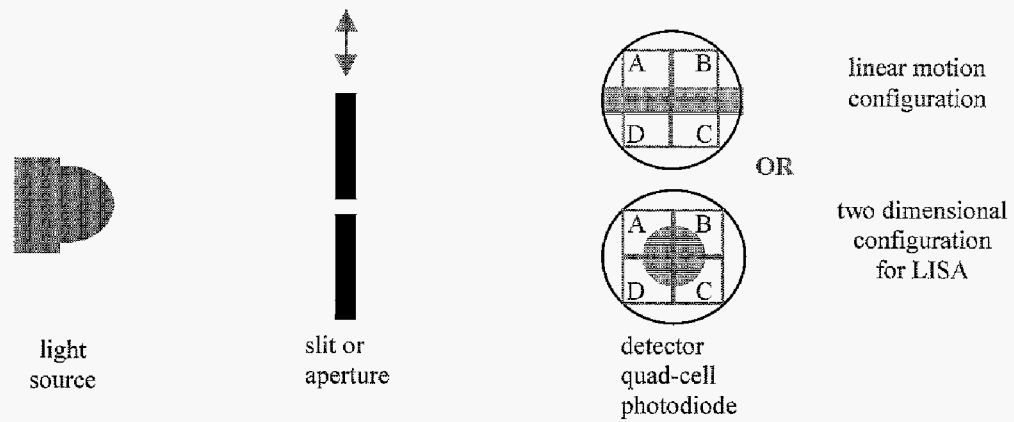


Fig. 1: A generic configuration for the optical displacement sensor (ODS).

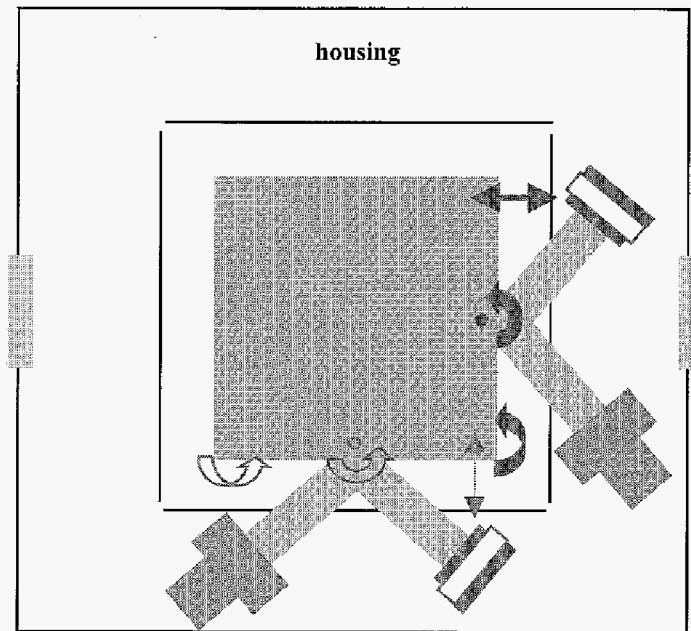


Fig. 2: Implementation configuration for LISA's application. For a definitive evaluation of relative displacements in all six degrees of freedom, three sets of ODS are suggested. Shown here are two sets and the monitored motions, and the third ODS is in the orthogonal direction to the page.

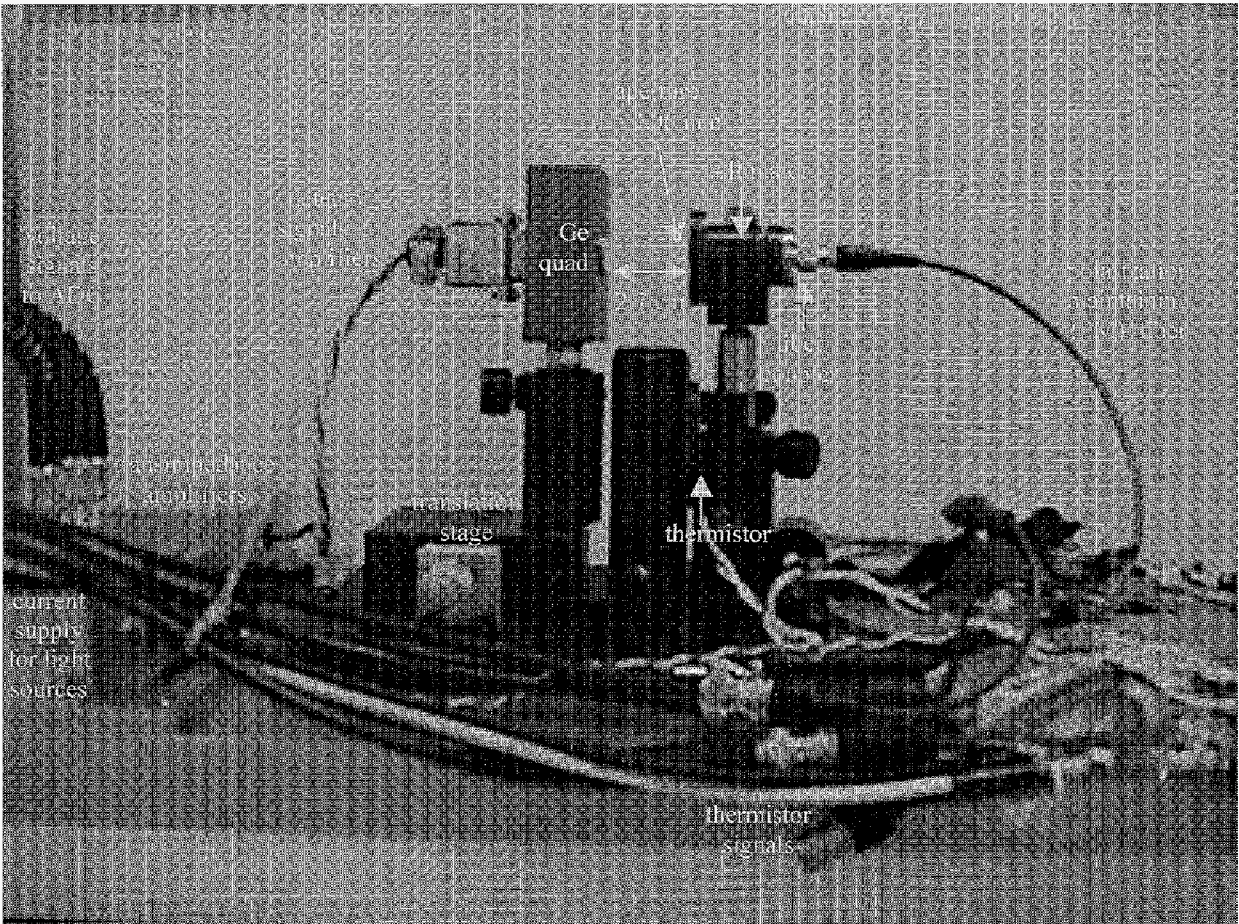


Fig. 3: A laboratory ODS setup inside the thermal insulation box.

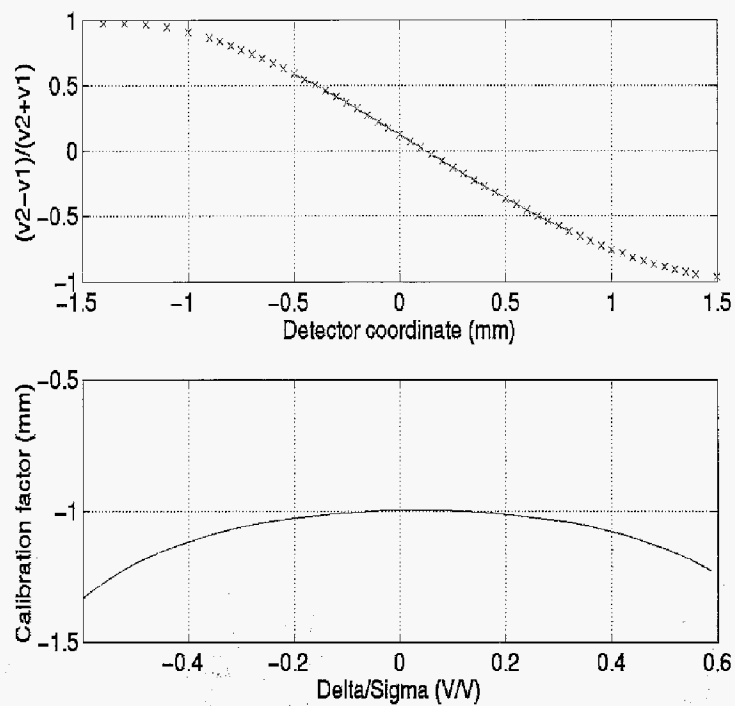


Fig. 4: A typical calibration data plot.

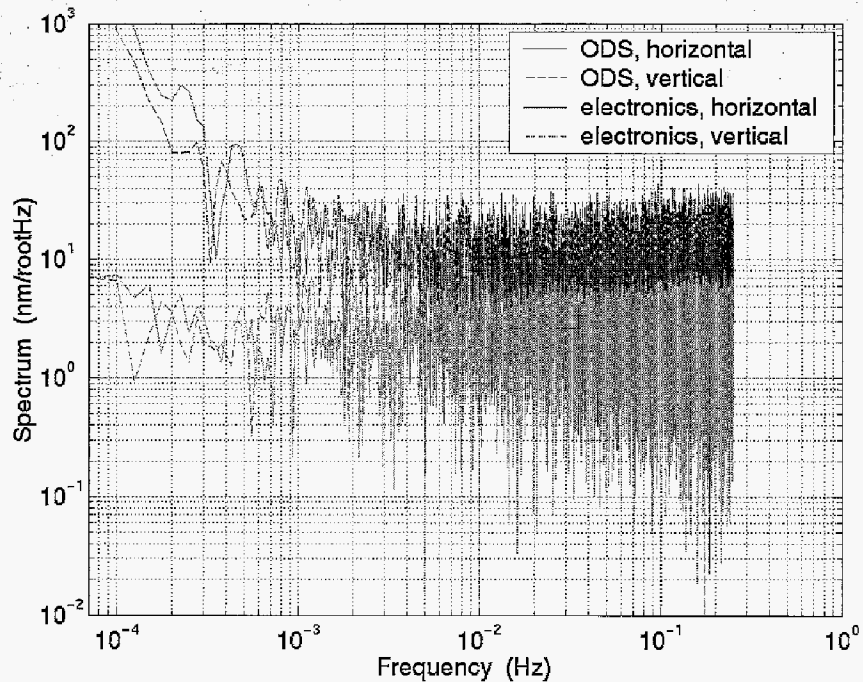


Fig. 5: A sample plot of ODS sensitivity and electronics noise measurements.